IEEE Robotics and Automation Letters (RA-L) paper, presented at ICRA 2026, Vienna, Austria. Cite as RA-L paper.

Torque Transmission Modeling of Two Coaxial Electrorheological Clutches for Reciprocating Actuation

Shouren Huang[1], *Member, IEEE*, and Masatoshi Ishikawa[1]

***Abstract*—This study focuses on modeling the transmission torque of two coaxial electrorheological (ER) fluid clutches through a data-driven approach. Instead of simplifying the viscosity term in the Bingham model to be a constant as shown in conventional methods, we propose the method of introducing electric field-dependent nonlinearity into the viscosity term to better capture the complex rheological behavior of ER fluids. Based on this framework, we developed a heuristic explicit model (HEM) and a radial basis function model (RBFM) that incorporate the mechanical characteristics of the coaxial clutch structure. Furthermore, we explored direct estimation methods using a radial basis function network (RBFN) and a feedforward neural network (FNN) without relying on the Bingham model. Comparative evaluations with traditional ER models validated the effectiveness of our nonlinear formulations. Notably, the FNN approach demonstrated superior accuracy even with a single hidden layer containing only a few neurons, making it well-suited for real-time implementation with minimal computational overhead. Real-time validation across diverse operating conditions further confirmed the feasibility and robustness of the FNN-based method. These findings contribute new insights into ER fluid applications.**

***Index Terms*—Actuation and Joint Mechanisms, Model Learning for Control, Dynamics, Electrorheological Fluid**

I. INTRODUCTION

RECIPROCATING actuation systems driven by electric motors are widely used in industrial and manufacturing applications, where frequent back-and-forth motion and repetitive start-stop operations are common. However, directly achieving reciprocating motion by controlling a motor's output direction presents several notable drawbacks. First, frequent motor reversals and start-stop operations can lead to significant motor degradation, including accelerated mechanical wear, thermal stress due to heat generation, electrical stress from inrush currents, and mechanical vibrations induced by dynamic loads. Second, gear backlash, which becomes prominent during motor reversal, introduces position errors and is especially problematic for robot systems [1].

Instead of directly controlling a driven motor to achieve high-speed reciprocating motion, employing clutches for bidirectional actuation presents a compelling alternative. By decoupling the motor from dynamic load reversals and enabling relatively steady unidirectional operation, mechanical and thermal stresses on the motor can be significantly reduced, thereby improving system reliability and extending operational lifespan. Furthermore, by eliminating motor reversals and introducing antagonistic driving, effects of gear backlash can be mitigated, leading to improved positioning accuracy and enhanced overall system performance. Clutches can be developed based on different methods, such as mechanical friction [2], magnetic particle [3], magnetorheological fluids [4]–[6], and electrorheological fluids [7]–[10]. Magnetorheological (MR) fluid clutches employ fluids that change viscosity in response to magnetic fields, allowing for adjustable torque transmission. Similarly, electrorheological (ER) fluid clutches use fluids that alter their rheological properties under electric fields, enabling controllable engagement and disengagement. Clutches based on mechanical friction are prone to significant wear, leading to reduced durability. Magnetic particle clutches and MR fluid clutches exhibit rate-dependent hysteresis, posing challenges for accurate modeling and control [11]. In contrast, ER fluid clutches, activated by electric fields, tend to exhibit less pronounced hysteresis effects [12], resulting in a simpler control model. This characteristic makes ER clutches easier to manage in applications that require precise torque control. Considering various advantages of ER fluid clutches, we designed a linear actuation system to achieve high-speed linear reciprocating motion utilizing two coaxial ER fluid clutches, as shown in Fig. 1. In addition to the advantages previously outlined, achieving reciprocating motion using ER clutches introduces hardware compliance, which contributes to safe interaction with the environment. Specifically, compared to pneumatic and hydraulic actuators, the proposed motor-driven linear actuation

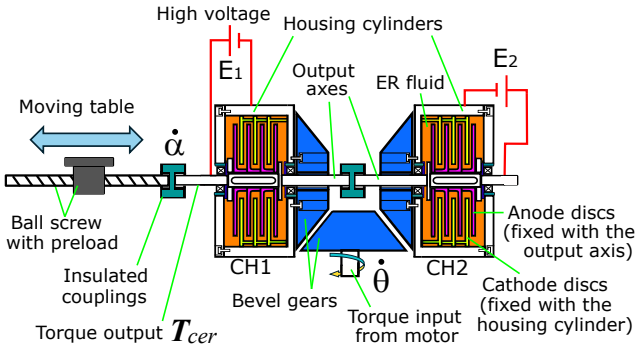

Fig. 1. Bidirectional linear actuation realized with two coaxial ER clutches. By modulating the rheological properties of the ER fluid between the anode and cathode discs through applied electric fields, the engagement and disengagement of the clutches are controlled to generate reciprocating motion. This study focuses on modeling the transmission torque T_{cer} produced by the two coaxial ER clutches.

Manuscript received: February, 16, 2025; Revised: July, 16, 2025; Accepted: October, 15, 2025.

This paper was recommended for publication by Editor Clement Gosselin upon evaluation of the Associate Editor and Reviewers' comments. This work was supported by the Grants-in-Aid for Scientific Research (KAKENHI)(22H03627, 23K24883) from the Japan Society for the Promotion of Science (JSPS). *(Corresponding author: Shouren Huang)*

[1]Shouren Huang and Masatoshi Ishikawa are with Research Institute for Science & Technology, Tokyo University of Science, Niijuku 6-3-1, Katsushika-ku, Tokyo, 125-8585, Japan. {huang,ishikawa}@ishikawa-vision.org

Digital Object Identifier (DOI): see top of this page.

IEEE Robotics and Automation Letters (RA-L) paper, presented at ICRA 2026, Vienna, Austria. Cite as RA-L paper.

system enjoys the advantages of fast response, good control accuracy, and lower power consumption [13]. On the other hand, solenoid-based electric actuators for linear reciprocating motion are generally constrained by short stroke lengths and are typically limited to simple on–off control.

In this study, we focus on modeling the transmission torque of the coaxial ER clutches, where the dynamic behavior of the ER fluid plays a critical role. The Bingham plastic model is commonly employed to characterize the dynamic behavior of ER fluids under applied electric fields [14].

$$\tau_{er} = \tau_y + \eta\dot{\gamma} \tag{1}$$

where, τ_y is the yield stress, η is the viscosity, $\dot{\gamma}$ is shear rate, and τ_{er} is the shear stress. The yield stress τ_y typically exhibits a power-law dependence on the electric field strength E, expressed as $\tau_y \propto E^{\beta}$, where β generally ranges from 1.0 to 2.0 [14]. The apparent viscosity η_a is then expressed by

$$\eta_a = \tau_y/\dot{\gamma} + \eta \tag{2}$$

We can see that if the second term η is treated as a constant, the nonlinearity of the electrorheological dynamics is reflected solely in the first term. The Bingham model provides a foundational understanding of ER fluid behavior. However, it may not fully capture the complex microstructural dynamics of ER fluids, particularly in cases where the ER fluid does not exhibit typical Bingham-like characteristics. To address these limitations, more advanced models, such as the six-parameter CCJ model [15] as well as the four-parameter SS model [16], have been proposed to incorporate the shear rate dependence into the yield stress term of the Bingham model. However, the incorporation of electric field-dependent nonlinearity into the viscosity term remains unexplored. Furthermore, practical applications of these models are hindered by challenges in parameter determination, sensitivity to parameter variations, and limited generalizability across different ER fluid systems.

Similar reciprocating mechanisms utilizing antagonistic MR and ER clutches have been investigated [6], [8]–[10]. In [8], ER actuators were treated as on–off devices by modeling the ER torque as a pure step function, and the relationship between shear stress and shear rate was assumed to be linear. The analog dynamic behavior of the ER fluid was not investigated. In [9], the transmission torque was approximated using a quadratic model with respect to electric field strength, and a first-order force response model as well as a second-order velocity response model were developed based on experimental studies. Similarly, in [10], the controllable torque of an ER clutch was modeled as a first-order system. These approaches rely on the assumption that the controllable transmission torque is solely a function of the electric field strength and the viscosity η in (1), (2) is simplified as a constant. Although this assumption may hold for ideal Bingham-like fluids under steady shear rate conditions, it is not generally valid, as demonstrated in [15], [16].

Rather than relying solely on theoretical analysis of rheological dynamics, data-driven approaches offer a promising alternative for capturing rheological behavior [17]–[21]. For instance, modeling and control with a data-driven approach for a two-speed magnetorheological fluid dual-clutch transmission system [17], using a neural network control scheme for a moving platform based on ER fluid valves [18], and modeling the yield stress of the ER fluid with a single hidden layer neural network [20], have been studied. Although extensive studies have explored the rheological behavior of various fluids using data-driven techniques, as summarized in [21], a significant gap remains in developing data-driven methods that achieve both real-time implementation and accurate torque transmission modeling for ER fluid actuators.

In this study, aiming for real-time applicability, we investigate several data-driven models to predict the transmission torque of two antagonistic ER clutches, without being constrained by the steady shear rate assumptions commonly adopted in prior work [8]–[10]. The main contributions of this work are twofold:

- We proposed the HEM and RBFM models to investigate the potential of more accurately capturing the dynamic behavior of ER fluids by modeling the dynamic viscosity term η as a nonlinear function of the electric field. Unlike conventional approaches [8]–[10], which simplify the nonlinear electrorheological dynamics by treating η as a constant, more advanced models [15], [16] provide improved representations of viscosity behavior. However, they still do not explicitly account for the electric field-dependent nonlinearity in the dynamic viscosity term. The proposed approaches demonstrated superior performance compared to previously mentioned methods and offer a novel perspective for ER fluid modeling.
- We proposed the RBFN and FNN approaches to model the electrorheological dynamics without relying on the Bingham model. We demonstrated that complex ER behavior can be effectively modeled using a simple feedforward neural network, even with only a few neurons. To the best of our knowledge, this study is the first to model the complex analog dynamic behavior of two antagonistic ER clutches using a neural network approach for real-time applications.

II. DEVELOPED SYSTEM

The overall structure of the developed system is shown in Fig. 2. Torque from a servo motor (HF-KP13, Mitsubishi Electric) is transmitted to the two ER clutches (maximum transmission torque: 0.5Nm, manufactured by ER Tech Co. Ltd.) via two sets of bevel gears both with 1:1 gear ratio.

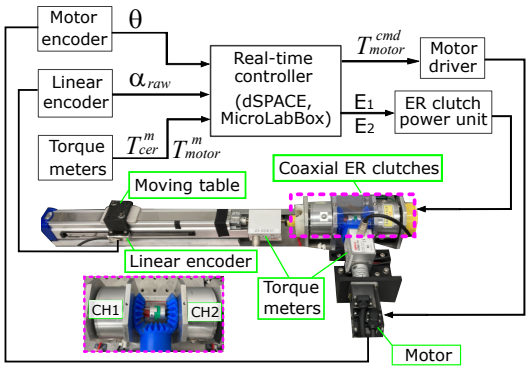

Fig. 2. Overview of the developed system.

IEEE Robotics and Automation Letters (RA-L) paper, presented at ICRA 2026, Vienna, Austria. Cite as RA-L paper.

TABLE I
RATED SPECS OF THE TWO ER CLUTCHES.

	Max. voltage (V)	Torque (N·m)	Current (mA)
CH1	2000	0.51	0.29
CH2	2000	0.48	0.27

Consequently, the housing cylinders of the two clutches, which are connected to the oppositely rotating bevel gears, rotate in opposite directions. The motor's rotation angle is measured by a 13-bit encoder. The output torque from the two coaxial ER clutches is recorded using a torque meter (UTMIII-0.5Nm, UNIPULSE CORPORATION). The position of the moving table is measured by a linear encoder (Q4BCX15D04A, RENISHAW PLC.) with 1μm resolution. A real-time controller (MicroLabBox, dSPACE GmbH) operates at 1 kHz control frequency. Additionally, another torque meter (UTMIII-5Nm, UNIPULSE CORPORATION) is used to measure the output torque from the motor. A ball screw with preload is employed to ensure minimal backlash and enhance positioning accuracy. The two ER clutches were designed to have multiple anode and cathode discs to increase the contact surface area, thereby enhancing torque transmission efficiency. The ER fluid consists of polymer particles containing sulfonic acid groups dispersed in a fluorinated medium. The sulfonic acid groups enhance particle polarizability, while the fluorinated medium ensures chemical stability and maintains appropriate viscosity. ER fluid is filled between the anode and cathode discs of the two clutches. By applying an electric field between the anode and cathode discs of either ER clutch, we can regulate bidirectional torque transmission to the ball screw linear actuator, which is connected to the output axis of both clutches. Specifically, when an electric field is applied to clutch CH2, the moving table of the ball screw linear actuator moves left, whereas applying an electric field to clutch CH1 causes it to move right. The rated specifications of the two ER clutches are listed in Table I.

III. TORQUE TRANSMISSION MODELING

The following two assumptions are established before we address the modeling of the transmission torque:

- Electric fields will not be applied to the two clutches simultaneously.
- The temperature variation of the ER fluid in both clutches is minimal, making the impact of electrorheological dynamics due to temperature changes negligible.

The first assumption is practical for applications, as stopping the linear actuation by simultaneously activating both coaxial clutches is neither optimal nor necessary. Regarding the second assumption, since both clutches have low power consumption (less than 0.6 W) and the housing cylinders are made of thin aluminum for improved heat dissipation, the temperature rise due to the applied electric field and kinetic energy conversion is negligible. We will provide supporting evidence in the experimental evaluations.

A. Problem Formulation

For ER fluid actuators, transmission torque is a primary performance metric. In a simplified model, where τ_{er}^{i} denotes the shear stress of a specific volume of ER fluid i, the transmission torque T_{er} can be expressed as

$$T_{er} = \int \tau_{er}^{i} \cdot r^{i} \cdot A^{i} \tag{3}$$

Here, the moment arm r^{i} and contact area A^{i} are parameters determined by the geometric structure of an ER actuator. Specifically, the torque transmission model of the two coaxial ER clutches defines a mapping function, denoted as $\mathscr{F}$, which describes the relationship between the applied electric fields (E_1, E_2 for ER clutch CH1 and CH2, respectively), the shear rates, and the resulting torque output T_{cer}. Specifically, the mapping function $\mathscr{F}$ encapsulates both the electrorheological dynamics and the geometric properties of the ER fluid clutches. The position of the moving table is measured as α_{raw}, and is nomalized as α to align with the motor's rotation angle θ, such that

$$\alpha = \alpha_{raw} \cdot 2\pi / p \tag{4}$$

where p is the lead of the ball screw. Consequently, the absolute value of the motor's velocity (which is the same as that of the housing cylinders of both ER clutches), $|\dot{\theta}|$, is equal to the absolute value of the linear actuator's velocity, $|\dot{\alpha}|$, when either one of the two clutches is fully activated by applying the maximum voltage. Otherwise, $|\dot{\theta}| > |\dot{\alpha}|$ holds. The shear rate magnitude of the ER fluid in each clutch is determined by the difference between $|\dot{\theta}|$, and $|\dot{\alpha}|$. Specifically, assuming that the housing cylinder of clutch CH1 rotates synchronously with the motor in the positive direction, the shear rate $\dot{\gamma}_1$ of the ER fluid between the anode disc and the cathode disc in clutch CH1 at a specific point i where its distance to the rotational center is r^{i}, can be expressed as

$$\dot{\gamma}_1^{i} = (\dot{\theta} - \dot{\alpha}) r^{i} \tag{5}$$

Similary, the shear rate $\dot{\gamma}_2$ of the ER fluid in clutch CH2 can be represented by

$$\dot{\gamma}_2^{i} = (-\dot{\theta} - \dot{\alpha}) r^{i} \tag{6}$$

(5) and (6) indicate that the shear rate is proportional to the relative angular velocity for each clutch. Therefore, in the modeling process, the shear rate will be represented by the corresponding relative angular velocity directly, such that $\dot{\gamma}_1 = (\dot{\theta} - \dot{\alpha})$ and $\dot{\gamma}_2 = (-\dot{\theta} - \dot{\alpha})$. The modeling objective is to establish the following relationship

$$T_{cer} = \mathscr{F}(E_1, E_2, \dot{\gamma}_1, \dot{\gamma}_2) \tag{7}$$

Note that the electric field inputs, E_1 and E_2, vary within the range [0, 0.5], and correspond linearly to the high voltage output range of [0V, 2000V] from the ER clutch power unit.

B. Data Collection

To excite a broad frequency range in the dynamics of the two ER clutches, electrical field inputs combining pseudorandom square and sinusoidal waves (frequency ranging from 2 to 100 Hz) were applied. Additionally, the motor torque command was configured as a pseudorandom square wave within a predefined range (amplitude: 0.04 to 0.15 Nm, frequency: 2 to 100 Hz). An example section of data samples,

IEEE Robotics and Automation Letters (RA-L) paper, presented at ICRA 2026, Vienna, Austria. Cite as RA-L paper.

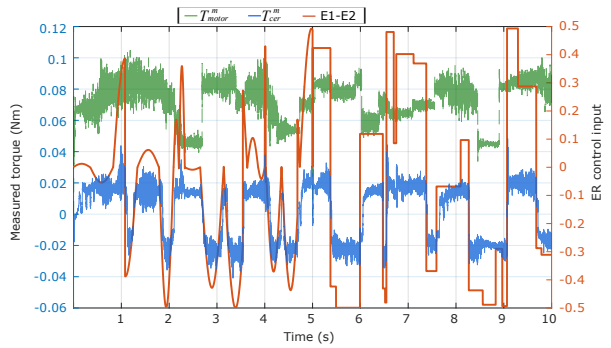

Fig. 3. A section of sample dataset with inputs and corresponding torque outputs.

containing electrical field inputs, output torque measurement of the two coaxial clutches, and motor torque measurement, is shown in Fig. 3. We collected a total of 290,000 samples with 1 ms sampling interval. Each sample comprises the electric field inputs E_1 and E_2, position values θ and α, and the output torque measurement T^m_{cer}.

C. Regression with a Heuristic Explicit Model (HEM)

Although the Bingham model in (1) provides a foundational framework to understand the behavior of ER fluids, its basic form is often adopted by simplifying the viscosity term η as a constant, as seen in prior studies [8]–[10]. Although more advanced models (e.g. [15], [16]), offer improved representations of nonlinear dynamics, they still do not explicitly incorporate electric field dependence into the dynamic viscosity term. Motivated by this limitation, we explore the possibility of more accurately capturing the dynamics of ER fluids by modeling the dynamic viscosity term η to reflect its nonlinear dependence on the electric field E. With the goal of minimizing the number of parameters needed to represent this nonlinear function, we express this relationship heuristically as

$$\eta = k(\beta_1 + e^{E\beta_2}) \tag{8}$$

where, k, β_1 and β_2 are design parameters. Based on the knowledge that the yield stress τ_y typically correlates with electric field E through a power-law relationship [14], we model it as a quadratic function. Therefore, transmission torque of a single ER clutch can then be represented as

$$T_{er} = k_1 E^2 sgn(\dot{\gamma}) + k_2(\beta_1 + e^{E\beta_2})\dot{\gamma} \tag{9}$$

Where, the regression parameters k_1 and k_2 represent the mechanical properties of a specific ER clutch. Although both clutches used the same type of ER fluid and had identical mechanical structures and dimensions, CH1 exhibited slight differences compared to CH2, as shown in Table I. Therefore, k_1 and k_2 account for the characteristic variations specific to each clutch. We then have the torque model of the two coaxial clutches as

$$\begin{aligned} T_{cer} &= T_{er1} + T_{er2} \\ &= a_1 E_1^2 sgn(\dot{\gamma}_1) + a_2(\beta_1 + e^{E_1\beta_2})\dot{\gamma}_1 \\ &\quad + b_1 E_2^2 sgn(\dot{\gamma}_2) + b_2(\beta_1 + e^{E_2\beta_2})\dot{\gamma}_2 \end{aligned} \tag{10}$$

where, a_1, a_2 are the regression parameters of CH1, and b_1, b_2 are that for CH2. Specifically, since $|\dot{\theta}| \geq |\dot{\alpha}|$ holds in this study, $sgn(\dot{\gamma}_1)$ is positive, while $sgn(\dot{\gamma}_2)$ is negative. By solving the following constrained optimization problem with a quadratic cost function that minimizes the difference between the model and the measured torque T^m_{cer} from the torque meter, we can estimate the parameters $a_1, a_2, b_1, b_2, \beta_1, \beta_2$.

$$\min_{a_1,a_2,b_1,b_2,\beta_1,\beta_2} |T_{cer} - T^m_{cer}|^2 \tag{11}$$

$$s.t.\ a_1 > 0, a_2(\beta_1 + 1) > 0, b_1 > 0, b_2(\beta_1 + 1) > 0$$

D. Regression with a Radial Basis Function Model (RBFM)

With the same consideration of modifying the dynamic viscosity term η by incorporating its nonlinear dependence on E, we can utilize the radial basis function (RBF) kernels to render the relationship as an alternative approach. The transmission torque for each clutch is represented as

$$T_{er} = k_0 E^2 sgn(\dot{\gamma}) + \dot{\gamma}\sum_{i=1}^{n} k_i e^{-\frac{(E-\mu_i)^2}{2\sigma_i^2}} \tag{12}$$

where, n represents the number of kernels, $k_0, k_{i=1,\ldots n}$ are regression parameters for a specific clutch. The center μ_i and the spread σ_i of the i-th kernel are defined as

$$\mu_i = \frac{i-1}{n-1} \cdot max(E),\ i = 1, 2, ..., n \tag{13}$$

$$\sigma_i = \sigma_1 + \frac{i-1}{n-1} \cdot (\sigma_2 - \sigma_1),\ i = 1, 2, ..., n \tag{14}$$

where, σ_1 and σ_2 are the lower and upper bounds of spread range. Here, considering $E \in [0, 0.5]$, we set them as 0.01 and 1.0, respectively.

We then have the transmission torque of two clutches as

$$\begin{aligned} T_{cer} &= a_0 E_1^2 sgn(\dot{\gamma}_1) + \dot{\gamma}_1 \sum_{i=1}^{n} a_i e^{-\frac{(E_1-\mu_i)^2}{2\sigma_i^2}} \\ &\quad + b_0 E_2^2 sgn(\dot{\gamma}_2) + \dot{\gamma}_2 \sum_{i=1}^{n} b_i e^{-\frac{(E_2-\mu_i)^2}{2\sigma_i^2}} \end{aligned} \tag{15}$$

Similary, the regression parameters for both clutches can then be estimated by solving the constrained optimization problem

$$\min_{a_0, a_{i=1,\ldots,n}, b_0, b_{i=1,\ldots,n}} |T_{cer} - T^m_{cer}|^2 \tag{16}$$

$$s.t. \sum_{i=1}^{n} a_i e^{-\frac{(-\mu_i)^2}{2\sigma_i^2}} > 0, a_0 > 0, \sum_{i=1}^{n} b_i e^{-\frac{(-\mu_i)^2}{2\sigma_i^2}} > 0, b_0 > 0$$

E. Regression with Radial Basis Function Networks (RBFN)

The HFM and RBFM approaches described above begin by modeling an individual ER clutch based on the Bingham model. The transmission torque of the system is then calculated by integrating the two clutches. Alternatively, we can directly estimate T_{cer} without explicitly modeling each clutch by using radial basis function networks (RBFN). Suppose the

IEEE Robotics and Automation Letters (RA-L) paper, presented at ICRA 2026, Vienna, Austria. Cite as RA-L paper.

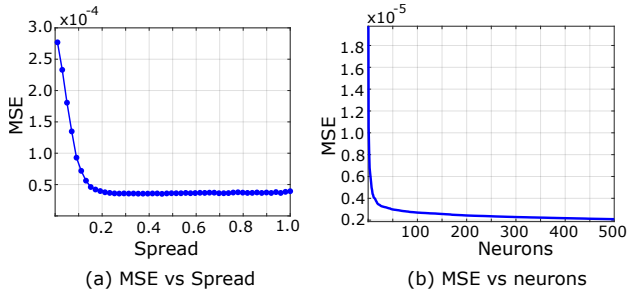

(a) MSE vs Spread (b) MSE vs neurons

Fig. 4. Regression loss related to the spread parameter as well as number of neurons for the RBFN approach.

hidden layer of the RBFN consists of n neurons, the model can then be expressed as

$$T_{cer} = \omega_0 + \sum_{i=1}^{n} \omega_i \phi(X) \tag{17}$$

Where, $\phi()$ is the Gaussion function, and the input X is as follows:

$$X = [E_1 - E_2, \dot{\gamma}_1, \dot{\gamma}_2]^T \tag{18}$$

The input feature $E_1 - E_2$ combines the electric field inputs for the two clutches based on the condition that they are activated with different timing. For implementation, all input features were normalized to the range [0,1]. The spread parameter, which controls the width of the radial basis functions and directly influences the network's generalization ability, was selected based on the value that yielded the lowest mean squared error (MSE), as shown in Fig. 4-(a).

F. Regression with Feedforward Neural Networks (FNN)

As an alternative to using RBF networks, we can also model the transmission torque with a simple feedforward neural network consisting of a single hidden layer with n neurons

$$T_{cer} = W_O \cdot tanh(W_I \cdot X + b_I) + b_O \tag{19}$$

where, $tanh()$ is the activation function, $W_I(n \times 3)$ represents the input weights, $b_I(n \times 1)$ denotes the input bias, $W_O(1 \times n)$ corresponds to the output weights, and $b_O(1 \times 1)$ is the output bias. Given the linear dependence of shear rates $\dot{\gamma}_1$ and $\dot{\gamma}_2$ on velocities $\dot{\alpha}$ and $\dot{\theta}$, we can directly use $\dot{\alpha}$ and $\dot{\theta}$ as input features for the neural network. Thus, the input is defined as

$$X = [E_1 - E_2, \dot{\theta}, \dot{\alpha}]^T \tag{20}$$

To achieve a good trade-off between model accuracy and simplicity, we examined the regression loss as the number of neurons increased. As shown in Fig. 5, using 16 neurons provided a well-balanced compromise between accuracy and model complexity.

A comparison of regression loss for different methods is presented in Table II using the same training and test datasets. All four proposed methods achieved higher accuracy than the Bingham basic model (with constant viscosity) and the SS model [16]. Specifically, for the RBFM method, performance stabilized with 10 kernels, and further increasing the number of kernels provided minimal improvement in regression error. For the RBFN method, the regression error decreases as the number of neurons increases, as shown in Fig. 4-(b). Overall, the

TABLE II
COMPARISON OF REGRESSION LOSS (MSE)

Approach	Train data	Test data
Bingham basic	9.3285e-05	1.8840e-04
SS model [16]	6.3870e-05	6.5099e-05
HEM	5.7981e-05	5.9232e-05
RBFM (5 kernels)	5.6833e-05	5.4622e-05
RBFM (10 kernels)	5.6757e-05	5.4524e-05
RBFN (10 neurons)	3.6013e-05	3.7933e-05
RBFN (50 neurons)	2.6146e-05	3.3274e-05
FNN (6 neurons)	2.1708e-05	1.8172e-05
FNN (16 neurons)	1.8542e-05	1.6703e-05
FNN (10, 6 neurons)	1.7718e-05	1.6382e-05

FNN method demonstrated the best performance, even with just 6 neurons, compared to other approaches. The last row in Table II presents the case of a feedforward neural network with two hidden layers (comprising 10 neurons in the first layer and 6 neurons in the second layer). The results indicate that using a single hidden layer in the FNN method provides a good balance between performance and computational cost. Plots of the predicted torque using different approaches are shown in Fig. 6-(a), with the corresponding test dataset illustrated in Fig. 6-(b). It is evident that the FNN method outperformed other approaches in capturing the electrorheological dynamics.

IV. REAL-TIME ONLINE VALIDATION

A. Implementation

Real-time online estimation of transmission torque was implemented using the FNN (16 neurons) method with the trained model parameters: input weights: $\hat{W}_I(16 \times 3)$, input bias: $\hat{b}_I(16 \times 1)$, output weights: $\hat{W}_O(1 \times 16)$, and the output bias: $\hat{b}_O(1 \times 1)$. Therefore, the torque estimation at time t is as follows:

$$\hat{T}_{cer}^t = \hat{W}_O \cdot tanh(\hat{W}_I \cdot X^t + \hat{b}_I) + \hat{b}_O \tag{21}$$

where, the input at time t is defined as

$$X^t = [E_1^t - E_2^t, \dot{\theta}^t, \dot{\alpha}^t]^T \tag{22}$$

where, $\dot{\theta}^t$ and $\dot{\alpha}^t$ represent the time derivatives of θ and α at time t. Normalization of the input data and denormalization of the estimation results were performed consistently with the procedures applied during the training process.

B. Torque Estimation under Predefined ER Control Inputs

The electric field inputs were configured as sinusoidal waves with random amplitudes and excitation durations within predefined ranges (amplitude: -0.5 to 0.5, frequency: 2 to

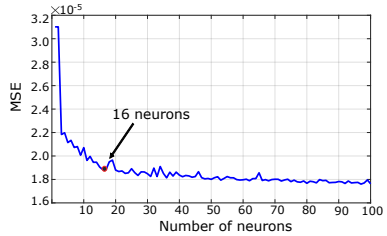

Fig. 5. Regression loss related to the number of neurons for the FNN approach.

IEEE Robotics and Automation Letters (RA-L) paper, presented at ICRA 2026, Vienna, Austria. Cite as RA-L paper.

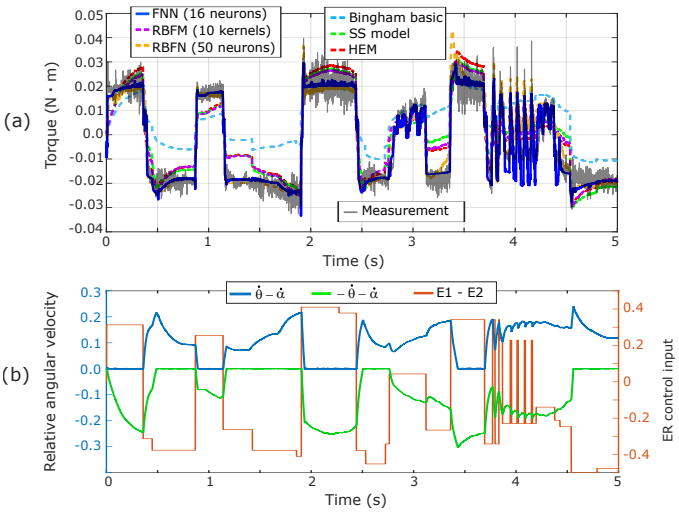

Fig. 6. Torque prediction under different methods. (a): Estimated torque profiles. (b): The corresponding ER control input and relative angular velocity profiles.

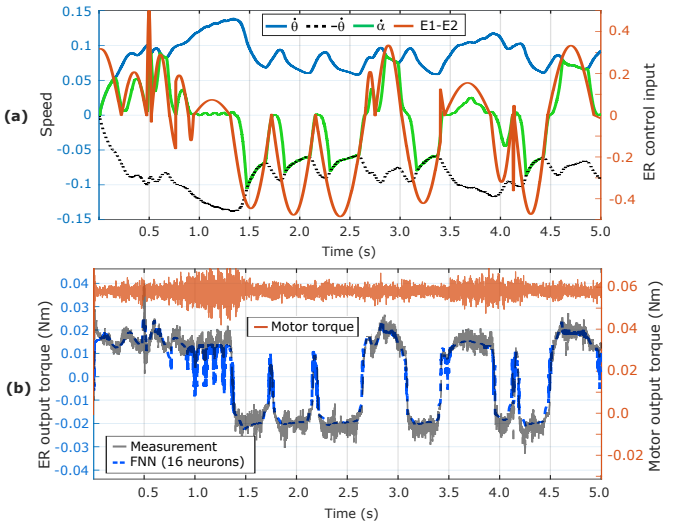

Fig. 7. Real-time online torque estimation under constant motor torque. (a): profiles of predefined input features; (b): torque profiles.

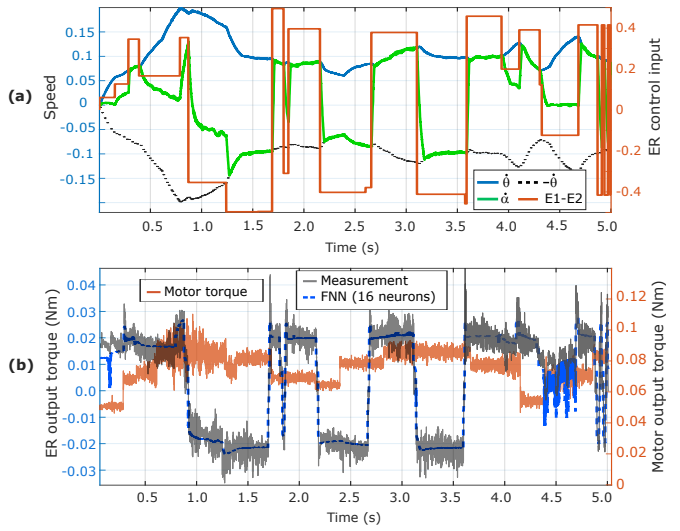

Fig. 8. Real-time online torque estimation under randomly variable motor torque. (a): profiles of predefined input features; (b): torque profiles.

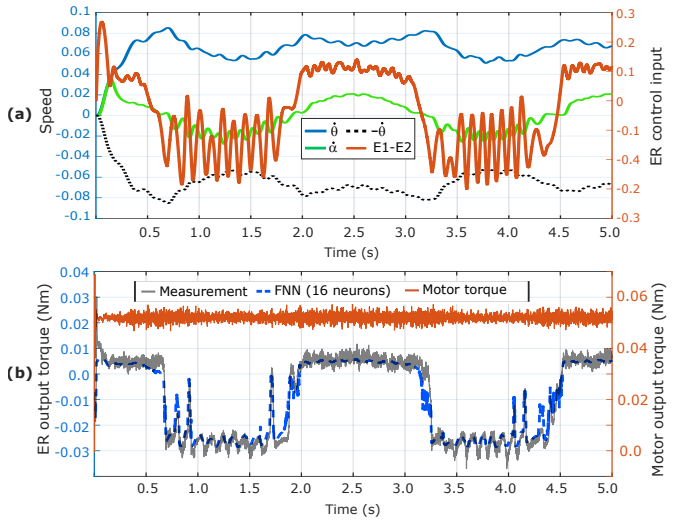

Fig. 9. Real-time online torque estimation under PD controlled position tracking at 0.4 Hz. (a): speed and ER control input profiles; (b): torque profiles.

100 Hz), while the motor torque was set to constant value. The results, shown in Fig. 7, demonstrate that the estimated torque values closely match the measured data. We then changed the electric field inputs to square waves with random amplitudes and excitation durations within predefined ranges (amplitude: -0.5 to 0.5, frequency: 2 to 100 Hz), and the motor torque was commanded to be pseudorandom square waves similarly (amplitude: 0.05 to 0.1 Nm, frequency: 2 to 100 Hz). Again, as shown in Fig. 8, the results demonstrate that the estimated torque values fit the measurement quite well.

C. Torque Estimation under Closed-Loop Tracking Control

To further validate the feasibility of the torque estimation model under more complex dynamic conditions, we implemented a closed-loop real-time tracking task, foregoing predefined electric field inputs to the two ER clutches. The position tracking of the linear actuator was achieved using a simple proportional-derivative (PD) controller as follows:

$$E = k_p \cdot (\alpha_r - \alpha) + k_d \cdot (\dot{\alpha}_r - \dot{\alpha}) \tag{23}$$

where, α_r is a reference trajectory of the linear actuator, k_p and k_d are gain coefficients. Since position control is not the primary focus of this study, the gain coefficients were not specifically tuned. We then set the inputs for the two ER clutches as: $E_1 = E,\ E_2 = 0$ for the case $E \geq 0$; and $E_1 = 0,\ E_2 = |E|$ for the case $E < 0$.

We implemented sine wave tracking at frequencies of 0.4 Hz and 2 Hz, each for 30 continuous trials sequentially (lasting for about 20 minutes in total), to assess the robustness of the model. The results for the first trial at 0.4 Hz and the last trial at 2 Hz are shown in Fig. 9 and Fig. 10, respectively. In both cases, the torque estimations closely matched the measurements, confirming the robustness of the model under continuous working conditions. During the tracking experiment, we also measured the temperature of the housing cylinder of clutch CH1 using a radiation thermometer (MT-11, MOTHERTOOL CO., LTD). The temperature variation was

IEEE Robotics and Automation Letters (RA-L) paper, presented at ICRA 2026, Vienna, Austria. Cite as RA-L paper.

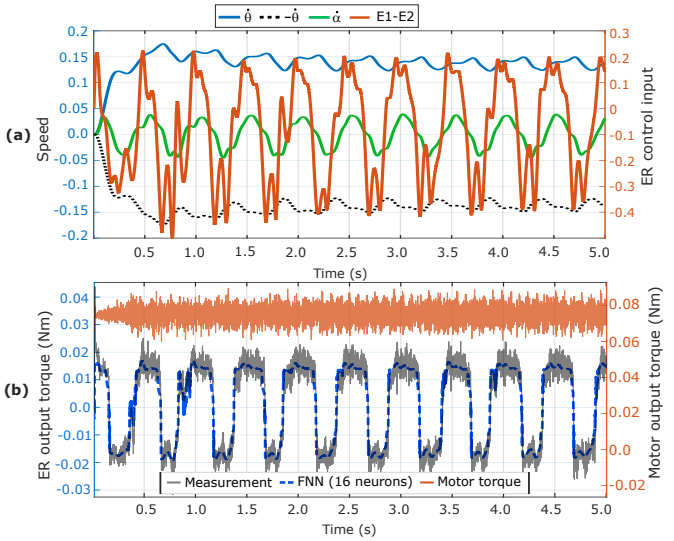

Fig. 10. Real-time online torque estimation under PD controlled position tracking at 2 Hz. (a): speed and ER control input profiles; (b): torque profiles.

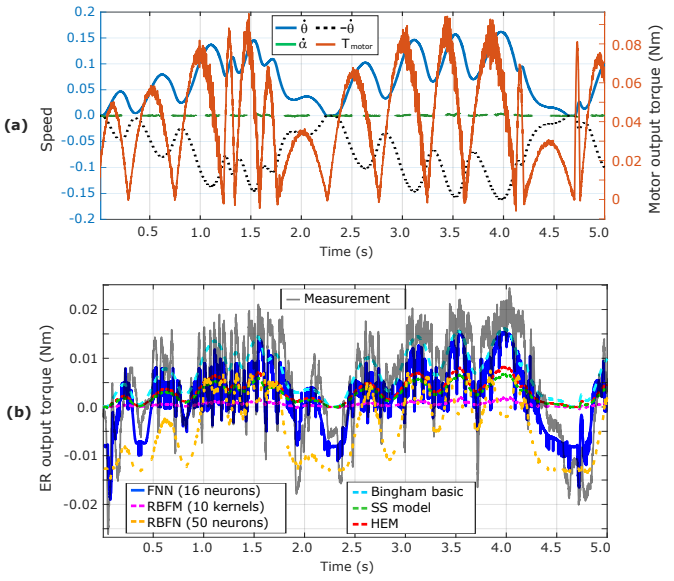

Fig. 11. Torque estimation under zero electric fields. (a): speed and motor torque profiles; (b): estimated torque profiles under different methods.

around $0.4^{\circ}C$, confirming that the temperature variation was minimal. This also aligns with our assumption regarding the temperature issue.

D. Torque Estimation under Zero Electric Fields

To validate the torque estimation models under zero yield stress conditions, we conducted evaluations with no electric fields applied to either of the two ER clutches. In this setup, the only control input was the motor torque command, which followed the positive half of a sine wave with randomly selected amplitude and frequency within a predefined range. Due to slight differences between the two ER clutches, the linear actuator exhibited limited motion. The estimation errors for different methods are summarized in Table III ($E_1 = E_2 = 0$), and the corresponding speed, motor torque, and estimated torque profiles are shown in Fig. 11. The results clearly demonstrate that the FNN method outperforms the others, closely matching the measured data. In particular, apart from the FNN method, the Bingham basic model yielded the best estimation accuracy among the remaining approaches. This suggests that these models incorporating nonlinear representations of dynamic viscosity are effective for modeling the rheological dynamics of ER fluids only when an electric field is applied.

TABLE III
TORQUE ESTIMATION ERRORS (MSE) UNDER ZERO ELECTRIC FIELD AND ZERO OUTPUT MOTION.

Approach	$E_1 = E_2 = 0$	$\alpha = 0$
Bingham basic	5.5329e-05	4.4685e-03
SS model [16]	7.3162e-05	2.5201e-03
HEM	6.5249e-05	2.2441e-03
RBFM (10 kernels)	1.0183e-04	2.0413e-03
RBFN (50 neurons)	9.7811e-05	3.4315e-03
FNN (16 neurons)	**4.0527e-05**	**1.9825e-03**

E. Torque Estimation under Zero Output Motion

To rule out the influence of disturbances caused by interactions with the load (i.e., the ball screw linear actuator) in previous evaluations, additional experiments were conducted with the output shaft of the two ER clutches held stationary. This setup represents a special case in which the relative angular velocities of the ER fluid in both clutches are equal in magnitude but opposite in direction. Estimation errors for different methods are summarized in Table III ($\alpha = 0$), and the corresponding profiles of speed, ER control input, and estimated torque are shown in Fig. 12. Note that the motor torque was applied as square waves with random amplitudes and excitation durations within predefined ranges (amplitude: 0.05 to 0.1 Nm, frequency: 2 to 100 Hz). Again, the FNN showed the best accuracy. In consistent with the evaluations under ball screw linear actuation, the HEM and RBFM methods outperformed both the Bingham basic model and the SS model, highlighting the effectiveness of introducing nonlinear dependence on the electric field into the dynamic viscosity. The RBFN method achieved higher accuracy than the Bingham basic model but lower accuracy than the SS model, indicating its inferior extrapolation capability compared to the FNN approach.

V. DISCUSSION

Although we have adopted a ball screw with preload to prevent backlash, it is still necessary to validate its impact in the experimental evaluations. To this end, a rotary encoder (MEH-30-6000PST5EF1(9), Microtech Laboratory Inc.) was installed on the output shaft of the two ER clutches (upstream of the ball screw) and compared against the linear encoder. As shown in Fig. 13, α measured by both encoders showed identical values. Furthermore, torque estimation with the FNN method showed consistent results. Therefore, the effect of ball screw backlash on the evaluations can be considered negligible.

VI. CONCLUSION

In this paper, we studied the torque transmission modeling of two coaxial ER clutches with four data-driven approaches.

IEEE Robotics and Automation Letters (RA-L) paper, presented at ICRA 2026, Vienna, Austria. Cite as RA-L paper.

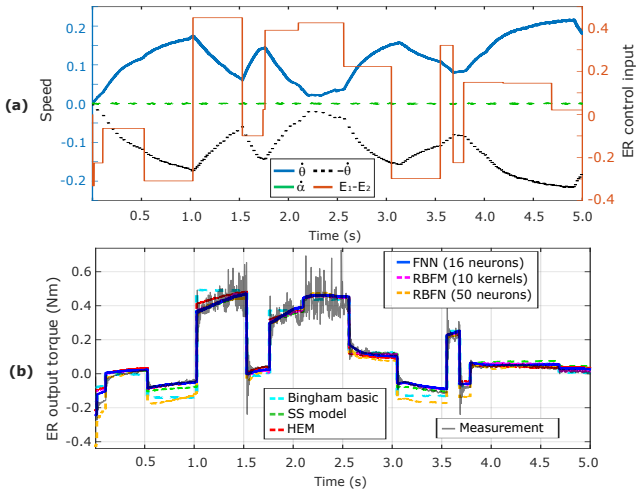

Fig. 12. Torque estimation with output axis fixed. (a): speed and ER control input profiles; (b): estimated torque profiles under different methods.

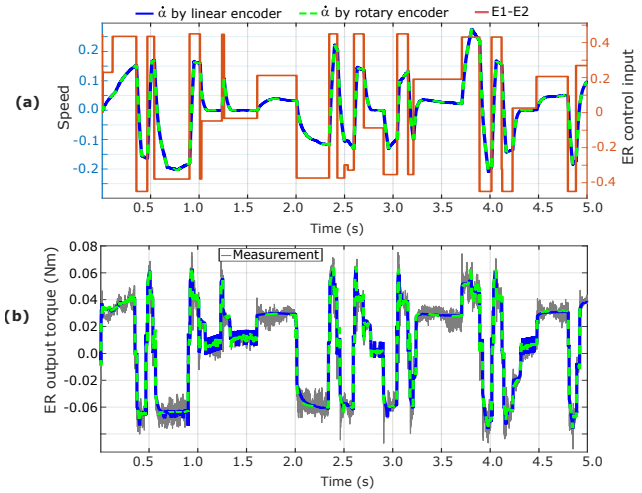

Fig. 13. Torque estimation comparison under the FNN method with α measured by a linear encoder and by a rotational encoder. (a): speed and ER control input profiles; (b): estimated torque profiles.

Traditional analytical methods typically employ geometric models of ER actuators, and rely on empirical models of simplified electrorheological dynamics that are limited to specific ER material properties. In contrast, our generalizable data-driven methodology derives a mapping function to encapsulate both the complex electrorheological dynamics and the geometric characteristics of the ER fluid system. In general, the proposed HEM and RBFM approaches demonstrated superior accuracy compared to the Bingham basic model and the SS model, indicating the benefits of incorporating the influence of applied electric fields into the dynamic viscosity term. However, their accuracy remained lower than that of the non-model-based FNN approach, even when the latter was implemented with a single hidden layer containing only a few neurons. This suggests that the limitations may arise either from the selected regression functions or from the inherent structure of the Bingham model. These findings contribute new insights into ER fluid applications.

REFERENCES

[1] K. Yong and C. G. Pickin, "Accuracy assessment of the modern industrial robot," *Industrial Robot*, vol. 27, no. 6, pp. 427–436, 2000.

[2] S. Kulkarni, A. Schmitz, S. Funabashi, and S. Sugano, "Development and evaluation of a linear series clutch actuator for vertical joint application with static balancing," in *2020 IEEE/RSJ International Conference on Intelligent Robots and Systems (IROS)*, 2020, pp. 6353–6360.

[3] P. H. Trickey and W. G. Martin, "The magnetic-particle power clutch," *Electrical Engineering*, vol. 70, no. 1, pp. 057–059, 1951.

[4] A. S. Shafer and M. R. Kermani, "On the feasibility and suitability of mr fluid clutches in human-friendly manipulators," *IEEE/ASME Transactions on Mechatronics*, vol. 16, no. 6, pp. 1073–1082, 2011.

[5] Y. Wang, A. Schmitz, K. Kobayashi, J. A. A. Lopez, W. Wang, Y. Matsuo, Y. Sakamoto, and S. Sugano, "Evaluation of series clutch actuators with a high torque-to-weight ratio for open-loop torque control and collision safety," *IEEE Robotics and Automation Letters*, vol. 3, no. 1, pp. 297–304, 2018.

[6] M. R. Kermani, S. Pisetskiy, I. Polushin, and Z.-Q. Yang, "Antagonistic magneto-rheological actuators with inherent output boundedness: An ideal solution for high-performance and human-safe actuation," in *Actuators*, vol. 12, no. 9. MDPI, 2023, p. 351.

[7] M. Whittle, R. Atkin, and W. Bullough, "Fluid dynamic limitations on the performance of an electrorheological clutch," *Journal of Non-Newtonian Fluid Mechanics*, vol. 57, no. 1, pp. 61–81, 1995, a selection of papers presented at an International Symposium on Viscoelastic Fluids.

[8] A. R. Johnson, W. A. Bullough, and J. Makin, "Dynamic simulation and performance of an electro-rheological clutch based reciprocating mechanism," *Smart Materials and Structures*, vol. 8, no. 5, p. 591, oct 1999.

[9] M. Sakaguchi, G. Zhang, and J. Furusho, "Modeling and motion control of an actuator unit using er clutches," in *Proceedings of IEEE International Conference on Robotics and Automation.*, vol. 2, 2000, pp. 1347–1353.

[10] S. B. Choi, S. S. Han, K. G. Sung, Y. S. Lee, and M. S. Han, "Accurate position tracking control of a moving stage using an electrorheological fluid clutch," *Smart Materials and Structures*, vol. 15, no. 3, pp. 850–858, may 2006.

[11] G. Chen, X. Xiong, Y. Lou, and Z. Li, "Modeling and observation of rate-dependent hysteresis and creep phenomena in magnetorheological clutch," *IEEE/ASME Transactions on Mechatronics*, vol. 27, no. 4, pp. 2053–2061, 2022.

[12] I. Chopra and J. Sirohi, "Electrorheological and magnetorheological fluids," in *Smart Structures Theory*, ser. Cambridge Aerospace Series. Cambridge University Press, 2013, p. 685–738.

[13] J. Pustavrh, M. Hočevar, P. Podržaj, A. Trajkovski, and F. Majdič, "Comparison of hydraulic, pneumatic and electric linear actuation systems," *Scientific Reports*, vol. 13, no. 20938, pp. 1–13, 2023.

[14] N. Kuznetsov, V. Kovaleva, S. Belousov, and S. Chvalun, "Electrorheological fluids: from historical retrospective to recent trends," *Materials Today Chemistry*, vol. 26, p. 101066, 2022.

[15] M. Cho, H. Choi, and M. Jhon, "Shear stress analysis of a semiconducting polymer based electrorheological fluid system," *Polymer*, vol. 46, no. 25, pp. 11 484–11 488, 2005.

[16] Y. P. Seo and Y. Seo, "Modeling and analysis of electrorheological suspensions in shear flow," *Langmuir*, vol. 28, no. 6, pp. 3077–3084, 2012.

[17] Y. Liang, J. Zhao, L. Deng, J. Zhao, P. K. Wong, and H. Du, "Investigation of data-driven modelling and feedforward control for a two speed magnetorheological fluid dual clutch transmission of electric vehicles," in *International Conference on Electric Vehicle and Vehicle Engineering (CEVVE 2023)*, vol. 2023, 2023, pp. 66–72.

[18] S.-B. Choi, K.-G. Sung, and J.-W. Lee, "The neural network position-control of a moving platform using electrorheological valves," *Journal of Dynamic Systems, Measurement, and Control*, vol. 124, no. 3, pp. 435–442, 07 2002.

[19] I. K. K. Scott A. Burton, Nicos Makris and P. J. Antsaklis, "Modeling the response of an electrorheological fluid damper: Constitutive models and neural networks," *Intelligent Automation & Soft Computing*, vol. 2, no. 4, pp. 339–354, 1996.

[20] K. Wei and G. Meng, "Yield stress modeling of electrorheological fluids using neural network," *International Journal of Modern Physics B*, vol. 19, no. 27, pp. 4093–4102, 2005.

[21] I. Bahiuddin, S. A. Mazlan, F. Imaduddin, M. I. Shapiai, Ubaidillah, and D. A. Sugeng, "Review of modeling schemes and machine learning algorithms for fluid rheological behavior analysis," *Journal of the Mechanical Behavior of Materials*, vol. 33, no. 1, p. 20220309, 2024.